Polyhedron 158 (2019) 225–233

Contents lists available at ScienceDirect

Polyhedron

journal homepage: www.elsevier.com/locate/poly

Azaallyl-derived ring formation via redox coupling in first row transition metals

Elliott B. Hulley, Spencer P. Heins, Peter T. Wolczanski *, Kyle M. Lancaster, Emil B. Lobkovsky

Department of Chemistry & Chemical Biology, Baker Laboratory, Cornell University, Ithaca, NY 14853, USA

ARTICLE INFO

Article history:
Received 16 August 2018
Accepted 30 October 2018
Available online 5 November 2018

Dedicated to Prof. William D. Jones, for his exemplary fundamental studies on bond activations, on the occasion of his 65th birthday; we greatly appreciate his mechanistic acumen and 43+ years of friendship.

Keywords:
Titanium
Azaallyl
Cyclopropane
Bond formation
Magnesium

ABSTRACT

The reductive coupling of a chelated diimine ligand, $Me_2C(CH{=}NCH_2(2\text{-py}))_2$ (dmp(PM)$_2$), by (TMEDA)$TiCl_2$ afforded a Ti(IV) species containing a cyclopropane ring, $Me^c_2Pr(cis\text{-}2,3\text{-}NCH_2(2\text{-py}))_2TiCl_2$ (**1**). Dimeric $[\{Me_2C(CH_2N{=}CH(2\text{-py})(CH_2(\mu\text{-}N)CH_2(2\text{-py})\}Mg]_2$ (**3**) was generated in the magnesium reduction of $Me_2C(CH_2N{=}CH(2\text{-py}))_2$ (dmp(PI)$_2$) as its reduction incurred HAT. A di-azaallyl precursor was used to generate 7-membered ring chelates $[\{DBM(PI^{-\cdot})(PI^{2-})\}Cr^{III}]_2$ (**4**) and $[\{DBM(PI)(PI')\}Fe]_2$ (**5**). Structural studies of **1**, **3** and **4** are included, as are electronic assessments of the reductive coupling to afford **1**, and the paramagnetism of **3**.

1. Introduction

In examining potential chelating ligands containing redox active components, azaallyl precursors were featured in a number of studies, and carbon–carbon bond formation was a key finding [1–8]. For example, the generation of azaallyls via deprotonation of $Me_2C(CH{=}NCH_2(2\text{-py}))_2$ (dmp(PM)$_2$) by $M\{NR_2\}_2(THF)_n$ (M = Cr, Co, R = TMS, n = 1–2; M = Ni, R = Ph, n = 0), led to the formation of three carbon–carbon bonds, setting six stereocenters in the process [1]. In a related study also shown in Fig. 1, pyrrolidines were catalytically synthesized in a complicated path involving azaallyl nucleophilic attack at a imine fragment [4], whereas the $Me_2C(CH_2N{=}CH(2\text{-py}))_2$ isomer failed to elicit any substantial chemistry.

Recently, the double-bond backbone of a $(dadi)^{4-}$ ligand (dadi = $[\{{-}CHN(1,2\text{-}C_6H_4)N(2,6\text{-}^iPr_2\text{-}C_6H_3)\}_2]^n$) attached to titanium was cyclopropanated by $PhHCN_2$ addition [9]. The reaction prompted the realization that ring generation via C—C bond formation might be a way of storing and releasing electrons if it were found to be reversible [10–19]. In this case, efforts failed to trigger the ring opening via the addition of various L, in part due to proton transfer, as exemplified in the formation of a nacnac-product generated when Ph_2CN_2 was utilized.

One means of providing a reversibly formed C—C bond, without interference from nacnac formation, is through use of a ligand with two non-hydrogen substituents on the mid-propyl carbon, such as dmp(PM)$_2$ [1,4]. Herein is presented evidence of cyclopropane formation via redox non-innocence (RNI), attempts at generating a magnesium version of the scaffold that could be used for metalations, and the generation of 7-membered rings with potential reversibility.

2. Results and discussion

2.1. $Me^c_2Pr(cis\text{-}2,3\text{-}NCH_2(2\text{-py}))TiCl_2$ (X = Cl, **1**; ^{neo}Pe, **2**)

2.1.1. Syntheses

Treatment of $(TMEDA)_2TiCl_2$ [20] with dmp(PM)$_2$ [1,4] in benzene led to the deposition of a crystalline red precipitate within 24 h. ^{1}H NMR spectroscopy revealed inequivalent methyls (δ 1.07, 1.59), diastereotopic methylene doublets (δ 4.61, 4.78, J = 21 Hz), and a 2H singlet at δ 3.13 in a region characteristic of cyclopropanes. The spectroscopic data implicated reduction of

* Corresponding author.
E-mail address: ptw2@cornell.edu (P.T. Wolczanski).

https://doi.org/10.1016/j.poly.2018.10.070
0277-5387/

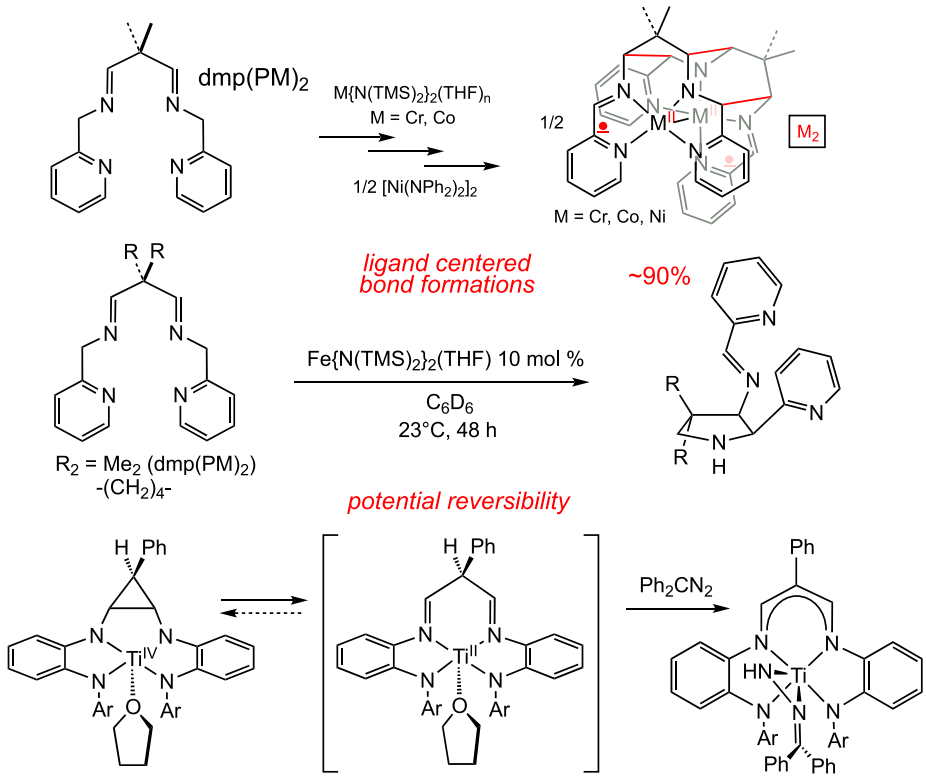

Fig. 1. Carbon–carbon bond-forming processes derived from $Me_2C(CH{=}NCH_2(2\text{-py}))_2$ including a cyclopropane ring-opening of a tetraamide titanium species derived from (dadi)^n.

the dmp(PM)$_2$ ligand by Ti(II) to afford the Ti(IV) dichloride, Me$^c_2$Pr(*cis*-2,3-NCH$_2$(2-py))TiCl$_2$ (**1**, 87%), as shown in Scheme 1.

Derivatization of dichloride **1** was accomplished on the NMR tube scale via the addition of two equiv of ^{neo}PeLi to afford the dialkyl Me$^c_2$Pr(*cis*-2,3-NCH$_2$(2-py))Ti(^{neo}Pe)$_2$ (**2**) in near quantitative yield. Two methyl groups were again observed by ^{1}H NMR spectroscopy at δ 1.27 and 1.57, along with diastereotopic methylene doublets (δ 4.76, 5.12, J = 21 Hz), a 2H singlet at δ 3.00, and typical neopentyl resonances. A related attempt at derivatizing **1** via the addition of Li{N(TMS)$_2$} led to an asymmetric complex suggestive of deprotonation of one 2-pyridyl-methyl arm of the chelate, but its subsequent thermolysis yielded a mixture of products, hence this avenue was discontinued. Attempts were also made to elicit similar reactivity from (TMEDA)$_2$VCl$_2$ [21]. Although the vanadium precursor reacted with dmp(PM)$_2$, the fate of the reactants could not be determined.

Several attempts were made to free the diamine chelate, Me$^c_2$Pr(*cis*-2,3-NHCH$_2$(2-py)), from the titanium so that it could be employed as a ligand in other systems. Simple hydrolysis, or acid- and base-hydrolyses, failed to generate the ligand scaffold without significant impurities. A switch to MeOH as the hydrolytic agent did not increase the amount of Me$^c_2$Pr(*cis*-2,3-NHCH$_2$(2-py)) formed, and did not appear to lessen the amount of impurity. As a consequence of these failures, quite possibly affected by the presence of Lewis acidic titanium components, other metals were sought to induce C—C bond formation.

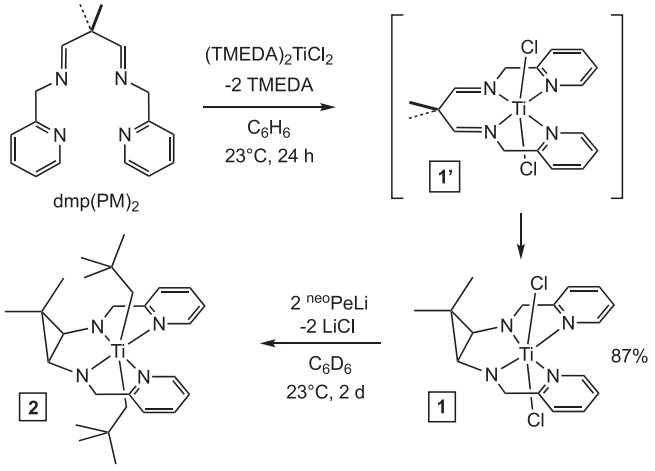

Scheme 1. Synthesis of Me$^c_2$Pr(*cis*-2,3-NCH$_2$(2-py))TiCl$_2$ (**1**) and derivatization to Me$^c_2$Pr(*cis*-2,3-NCH$_2$(2-py))Ti(^{neo}Pe)$_2$ (**2**).

2.1.2. Structure of Me$^c_2$Pr(*cis*-2,3-NCH$_2$(2-py))TiCl$_2$ (**1**)

As the molecular view in Fig. 2 confirms, the 1,3-diimine feature of the dmp(PM)$_2$ ligand has been converted to a cyclopropane via reduction by the titanium center to afford Me$^c_2$Pr(*cis*-2,3-NCH$_2$(2-py))TiCl$_2$ (**1**). In the process, the imines are now amides, and their 1.9351(7) Å (ave) distance is clearly shorter than the d(TiN) of the pyridines at 2.2570(23) Å (ave). The overall symmetry of **1** is approximately C_s, and the geometry of the 6-coordinate complex is severely distorted from octahedral, with the two chlorides leaning (∠Cl1—Ti—Cl2 = 133.93(2)°, ∠Cl1—Ti—N1,N4 = 81.455(7)° (ave), ∠Cl2—Ti—N1,N4 = 81.03(21)° (ave)) into the open pocket (∠N1—Ti—N4 = 134.21(4)°) of a planar N$_4$-titanium unit (Σ(∠NTiN) = 360.03°). The *cis*-diamide bite angle is ∠N2—Ti—N3 = 77.96(5)°, while the remaining amide-pyridine arms of the chelate have NN-bite angles that average 73.93(14)°. The cyclopropane is somewhat asymmetric as the C—C bond lengths affiliated with the dimethyl unit are 1.531(2) Å (ave), compared to the remaining d(CC) of 1.492(2) Å pertaining to the diamide carbons [22]. If the standard BDE vs. d(CC) holds,[23] the

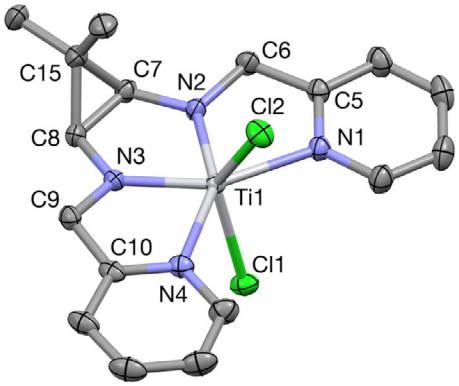

Fig. 2. Molecular view of Me$_2^S$Pr(*cis*-2,3-NCH$_2$(2-py))TiCl$_2$ (**1**). Selected interatomic distances (Å) and angles (°): Ti—N1, 2.2586(12); Ti—N2, 1.9356(11); Ti—N3, 1.9346 (12); Ti—N4, 2.2553(11); Ti—Cl1, 2.3690(4); Ti—Cl2, 2.3672(5); N1—C5, 1.3382(17); C5—C6, 1.489(2); N2—C6, 1.4522(17); N2—C7, 1.4341(18); C7—C8, 1.4916(19); C7—C15, 1.530(2); C8—C15, 1.5323(19); N3—C8, 1.4375(17); N3—C9, 1.4551(17); C9—C10, 1.489(2); N4—C10, 1.3369(19); N1—Ti—N2, 73.83(4); N1—Ti—N3, 151.75 (4); N1—Ti—N4, 134.21(4); N2—Ti—N3, 77.96(5); N2—Ti—N4, 151.95(5); N3—Ti—N4, 74.03(5); Cl1—Ti—N1, 81.45(3); Cl1—Ti—N2, 108.10(4); Cl1—Ti—N3; 106.38(4); Cl1—Ti—N4, 81.46(3); Cl2—Ti—N1, 80.88(3); Cl2—Ti—N2, 107.15(4); Cl2—Ti—N3, 109.20(4); Cl2—Ti—N4, 81.19(3); Cl1—Ti—Cl2, 133.93(2).

latter CC bond is ~16 kcal/mol stronger (108 vs. 92 kcal/mol) than those to the unique dimethylcarbon.

2.1.3. Calculations of Me$_2^S$Pr(*cis*-2,3-NCH$_2$(2-py))TiCl$_2$ (*1*)

Cyclopropane formation [16–19,24–28] can be viewed as an initial chelation to afford a formal Ti(II) derivative, {dmp(PM)$_2$}TiCl$_2$ (**1′**), followed by reduction of the diimine functionality [1,4,29–32]. Concomitant rotation of the requisite CHCMe$_2$CH fragment and ring closure affords the cyclopropanated Me$_2^S$Pr(*cis*-2,3-NCH$_2$(2-py))TiCl$_2$ (**1**). The reverse of this process illustrates how the C—C bond formation could mediate redox non-innocent transformations. Fig. 3 illustrates a truncated MO diagram of **1**, revealing 2 electrons in a C—C bonding orbital of low energy, and empty d-orbitals, one which is spread over two mixed orbitals that are roughly equal in titanium and ligand composition. When the cyclopropane is opened to the minimized diimine **1′**, two orbital pairs each share one d-orbital, and one of mixed composition contains a single electron and is ~45% titanium. A second electron resides in another d-orbital that is ~70% titanium in character, and both singly occupied MOs are ~3.5 eV above the C—C bonding orbital in **1**.

Fig. 4 indicates that a substantial energy penalty (~14 kcal/mol) is paid upon ring opening the cyclopropane in Me$_2^S$Pr(*cis*-2,3-NCH$_2$(2-py))TiCl$_2$ (**1**), mostly due to the difference in energy of the HOMOs illustrated in Fig. 3 (~7.0 eV), which are not compensated enough in the construction of two imine π-bonds and the accompanying minor structural and electronic changes. There is a modest kinetic barrier to the ring opening due to the reorientation of the CHCMe$_2$CH moiety, and the unrestricted configuration is a triplet slightly below its broken symmetry configuration (BS 1,1) in energy. The unrestricted and BS solutions are ~10 and ~6 kcal/mol below the restricted singlet in energy. The calculations clearly show that the utilization of a reversible C—C bond formation in a redox non-innocent capacity has potential, but perhaps not in this relatively crowded titanium system, with its energy penalty.

2.2. Magnesium reduction of dmp(PM)$_2$ and dmp(PI)$_2$

2.2.1. Synthesis of [{Me$_2$C(CH$_2$N=CH(2-py)(CH$_2$(μ-N)CH$_2$(2-py)}Mg]$_2$ (*3*)

Cyclopropane formation via dmp(PM)$_2$ was sought with typical reducing agents that might benefit from chelation subsequent to electron transfer. Unfortunately, exposure of dmp(PM)$_2$ to Zn°, Mg°, Mg°/HgCl$_2$, and Sn° under various conditions failed to elicit any sign of reduction. Given the propensity of iminopyridine functionalities to become reduced by 1 or 2 electrons, the dmp(PI)$_2$ isomer [29] was examined in view of previous comparative studies with iron [4]. Treatment of (TMEDA)$_2$TiCl$_2$ with dmp(PI)$_2$, as shown in Scheme 2, did not lead to a stable {dmp(PI$^{-\cdot}$)$_2$}Ti^{IV}Cl$_2$ complex as expected. Instead, decomposition consistent with chelate

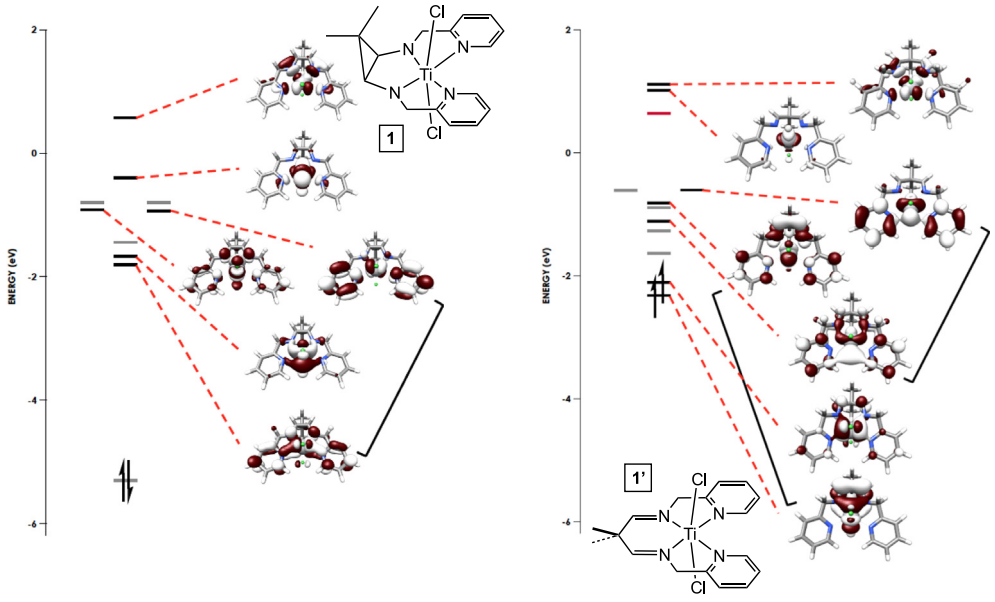

Fig. 3. Truncated MO diagrams illustrating metal (black) and ligand-dominated (gray) orbitals: (a) spin restricted B3LYP MOs for Me$_2^S$Pr(*cis*-2,3-NCH$_2$(2-py))TiCl$_2$ (**1**) with d(CC) = 1.45 Å; a pair of orbitals shown via the black tie-bar indicate combinations with the same d-orbital; (b) quasi-restricted B3LYP MOs for hypothetical {dmp(PM)$_2$}TiCl$_2$ (**1′**) with d(CC) = 2.45 Å, singly occupied d-orbitals that are 45% and 70% titanium in character, and two orbital combinations connected by tie-bars that each use the same d-orbital. Orbitals are plotted at an isovalue of 0.03 au.

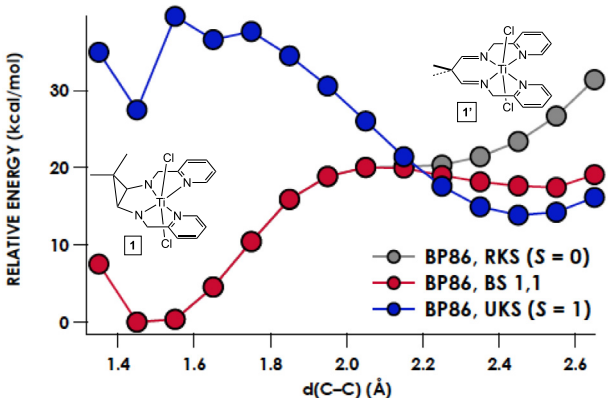

Fig. 4. Energy changes (kcal/mol) as the Ti(IV) cyclopropane derivative Me_2^sPr(*cis*-2,3-NCH_2(2-py))$TiCl_2$ (**1**) ring-opens to its Ti(II) isomer, {dmp(PM)$_2$}$TiCl_2$ (**1′**), which was treated as a restricted singlet (gray), calculated using broken symmetry (BS 1,1, red) and as a spin-unrestricted triplet (blue). (Color online.)

reduction was observed, and synthetic variations, such as $TiCl_3$(-THF)$_3$ with 1 equiv of reducing agent, led to similar results.

The failure to generate a titanium complex with reduced iminopyridine moieties prompted a switch to main group reductants, and Mg° [33] (w trace $HgCl_2$) afforded a black/red material after 2d at 23 °C. Yields of the material varied greatly, and diamagnetic resonances were absent in its ^{1}H NMR spectrum, aside from typically small amounts of dmp(PI)$_2$. Evans' method [34] measurements of the presumed "{dmp(PI$^{-\cdot}$)$_2$Mg" product consistently found μ_{eff} to be 1.3–1.4 μ_B. This value is inconsistent with a plausible $S = 1$ center, hence crystals were obtained for X-ray analysis, and the complex was discovered to be a dimer, [{dmp(PI$^{-\cdot}$)(μ-NPM)}Mg^{II} (**3**), in which hydrogen atom transfer (HAT) had occurred. As a dimer, the μ_{eff} of 1.8–2.0 (μ is proportional to $(1/c)^{1/2}$, where c = concentration; since c is halved as a dimer, its μ_{eff} is $(2)^{1/2}$ times that of a monomer) is consistent with two $S = 1/2$ centers possessing some antiferromagnetic coupling (if no coupling, $\mu_{eff} = g[S_a(S_a + 1) + S_b(S_b + 1)]^{1/2}\mu_B = 2.45$ μ_B) [35]. The methine centers in which the radical character has the greatest magnitude are 8.047 Å apart, thus it is likely the diamond core aids the coupling.

2.2.2. Structure of [{Me_2C(CH_2N=CH(2-py)(CH_2(μ-N)CH_2(2-py)}Mg]$_2$ (**3**)

Fig. 5 illustrates the centrosymmetric dimer (C_i) containing a chelate that has a hydrogen atom added to one arm of the tetradentate dmp(PI)$_2$ ligand. As a consequence, one of the iminopyridine units has been converted to —(μ-N)CH_2(2-py), and its amide nitrogen now bridges the magnesiums. The coordination geometry about each Mg is a distorted trigonal bipyramid ($\tau = 0.58$),[36] with a nearly square $Mg_2(\mu\text{-}N)_2$ core (∠N2—Mg—N2′ = 91.48(4)°; ∠Mg—N2—Mg = 88.52(4)°), and N_{ax}—Mg—N_{ax} angle of 168.39(5)°. The d(MgN_{im}) distance of 2.0724(12) Å is shorter than the axial (2.1108(11) Å) and equatorial (2.1124(12) Å) nitrogens of the μ-amides, and considerably shorter than the pyridine d(MgN) of 2.1657(12) Å. The methylene derived from the PI unit is readily identified by its ∠N2—C6—C5 = 113.41(11), and d(CN) and d(CC) distances of 1.4552(18) Å and 1.506(2) Å, respectively. Contrast these metric parameters with those of the reduced iminopyridine, whose d(N_{im}C) = 1.3191(18), d(CC) = 1.4134(19), and d(N_{py}—C) = 1.3840 (17) are typical for a radical anion [29–32].

2.2.3. Electronic structure of [{Me_2C(CH_2N=CH(2-py))(CH_2(μ-N)CH_2(2-py))}Mg]$_2$ (**3**)

Broken symmetry DFT calculations on [{Me_2C(CH_2N=CH(2-py))(CH_2(μ-N)CH_2(2-py))}Mg]$_2$ (**3**) are consistent with its observed magnetism, as Fig. 6 illustrates magnetic orbitals that are essentially free of overlap. Calculations of the complex reveal the singlet/triplet gap to be also essentially zero, and the triplet state is favored by a mere $J = -1.8$ cm^{-1}. Since this is well below the accuracy of the calculations, it is possible that **3** is slightly antiferromagnetic, given the slightly less than spin-only values of μ_{eff} = 1.8–2.0 μ_B.

2.3. 7-Membered ring formation via 2-azaallyl coupling

2.3.1. Synthesis of a di-2-azaallyl tetradentate ligand

The synthesis of larger rings other than the previously examined 3- [9], 5- [4], and 6-membered ones [1] was envisaged to occur from particular 2-azaallyl precursors [1,2,4,37,38]. Methylene-*bis*-(4-(tert-butyl)-2-methyl-6,1-phenylene))bis(methanylylidene))bis(1-(pyridin-2-yl)methanamine (DBM(PM)$_2$H$_2$) was an

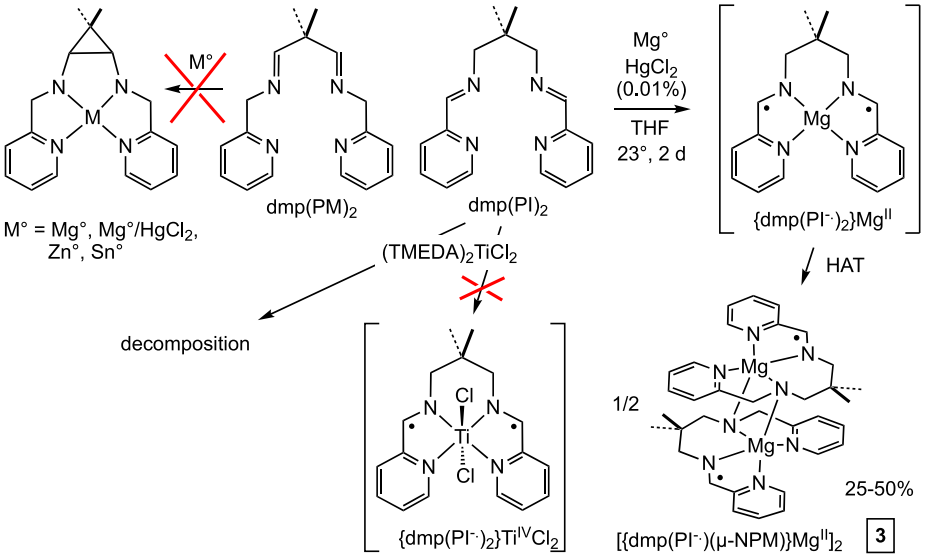

Scheme 2. When dmp(PM)$_2$ main group reductions failed, Mg° reduction of its iminopyridine isomer led to HAT and dimer formation.

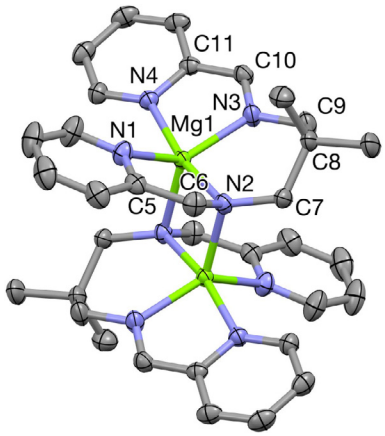

Fig. 5. Molecular view of [{$Me_2C(CH_2N{=}CH(2\text{-py})(CH_2(\mu\text{-}N)CH_2(2\text{-py})\}Mg]_2$ (**3**). Selected interatomic distances (Å) and angles (°): Mg1—N1, 2.1657(12); Mg1—N2, 2.1108(11); Mg1—N2′, 2.1124(12), Mg1—N3, 2.0724(12); Mg1—N4, 2.1657(12); N1—C5, 1.3435(18); C5—C6, 1.506(2); N2—C6, 1.4552(18); N2—C7, 1.4660(16); C7—C8, 1.5524(19); C8—C9, 1.538(2); N3—C9, 1.4435(18); N3—C10, 1.3191(18); C10—C11, 1.4134(19); N4—C11, 1.3840(17); Mg1—Mg1′, 2.9473(8); N1—Mg1—N2, 79.89(5); N1—Mg1—N2′, 106.23(5); N1—Mg1—N3, 133.40(5); N1—Mg1—N4, 100.31 (5); N2—Mg1—N2′, 91.48(4); N2—Mg1—N3, 92.77(5); N2—Mg1—N4, 168.39(5); N3—Mg1—N2′, 120.01(5); N3—Mg1—N4, 78.60(5); N4—Mg1—N2′, 99.54(4); Mg1—N2—Mg2, 88.52(4); N2—C6—C5, 113.41(11); N2—C7—C8, 117.85(11); N3—C9—C8, 113.85(12); N3—C10—C11, 119.60(12).

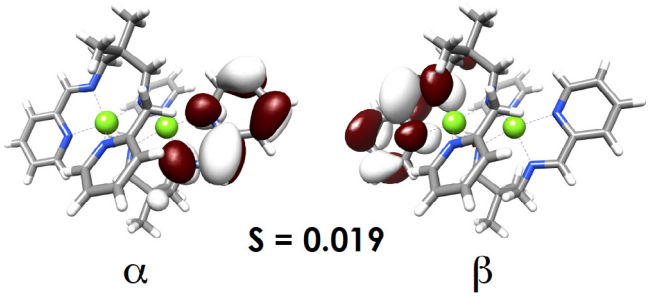

Fig. 6. Unrestricted corresponding magnetic orbitals of [{$Me_2C(CH_2N{=}CH(2\text{-py})(CH_2(\mu\text{-}N)CH_2(2\text{-py})\}Mg]_2$ (**3**), showing essentially zero overlap. Orbitals are plotted as an isovalue of 0.03 au.

attractive target, since the diphenol starting material was readily available [39]. As Scheme 3 indicates, its conversion to the di-triflate, followed by palladium-catalyzed cyanation, afforded a di-cyanide that was transformed to a di-aldehyde by conventional DIBAL-H reduction and hydrolysis. Condensation with 2-aminomethylpyridine generated $DBM(PI)_2$, a ligand whose imines could be reductively coupled to produce a 7-membered ring, or be activated by basic substrates to provide products derived from the incipient 2-azaallyl functionality.

2.3.2. Synthesis of [{$DBM(PI)_2$}M]$_2$ (M = Cr, Fe)

Attempts to metalate $DBM(PM)_2H_2$ were initiated with $Cr(N(TMS)_2)_2(thf)_2$ [40], whose basic amides had been shown to deprotonate azaallyls in previous work (Fig. 1). Alternatively, the Cr(II) center might be a potent enough reductant to simply couple the diimine unit. The addition of $Cr(N(TMS)_2)_2(thf)_2$ to 1 equiv $DBM(PM)_2H_2$ resulted in a color change from lavender to deep red and the evolution of THF and HMDS in a 1:1 ratio, as monitored by ^1H NMR spectroscopy over 1–2 d at 23 °C. There were no identifiable paramagnetic products at any stage in the process. A modest scale-up of this reaction in benzene allowed the isolation of a new complex as a dark red powder in 67% yield, and crystals suitable for X-ray analysis were grown from THF at −40 °C.

As shown in Scheme 4, the red complex was determined to be a dimer, formulated as [{$DBM(PI^{-\cdot})(PI^{2-})\}Cr^{III}]_2$ (**4**), in which one iminopyridine is a radical anion, and the second is doubly reduced to a azametalcyclopropane. In the process of deprotonating the 2-azapropene unit, a *cis*-carbon–carbon bond formation has occurred to generate the expected 7-membered ring. The dichromium unit remains paramagnetic, and the μ_{eff} at 298 K is 3.8 μ_B by Evans' method [34]. Two uncoupled Cr(III) $S = 3/2$ centers would be expected to possess a moment (i.e., $\mu_{eff} = g[S_a(S_a + 1) + S_b(S_b + 1)]^{1/2}\mu_B$) of about 5.5 μ_B, whereas coupled centers could be diamagnetic ($\mu_{eff} = 0$) to ~6.9 μ_B (i.e., $2[(3(3 + 1)]^{1/2}\ \mu_B$). The measured value is consistent with a dichromium interaction with sufficient antiferromagnetic coupling to attenuate its moment, but not enough coupling to render a diamagnetic complex.

The reaction of $DBM(PM)_2H_2$ with $Fe(N(TMS)_2)_2(thf)$ [41] was conducted in C_6D_6 on an NMR tube scale for convenient monitoring. The green color rapidly gave way to red-brown, and the presence of THF and HMDS were observed in a 1:1 ratio amidst paramagnetic resonances. After two days at 23 °C, a substantial amount of diamagnetic material was noted and after 8 d, >80% conversion to this red product was noted. Attempts to grow X-ray quality crystals of the material were not fruitful, so multiple 2D NMR techniques were utilized to provide a connectivity and basic structure to the complex.

A $^1H/^{13}C$ HSQCAD experiment correlated the hydrogens with their respective carbons, whereas a gCOSY experiment provided a correlation between adjacent hydrogens. The crucial COSY interaction related hydrogens at δ 6.36 and δ 5.20, which comprise the two benzylic carbons that are connected in the dibenzocycloheptane ring, and the *cis*-stereochemistry of the ring junction. In addition, hydrogens of the two pyridine imines are distinct, with one possessing shifts in close agreement with free ligand, and the other

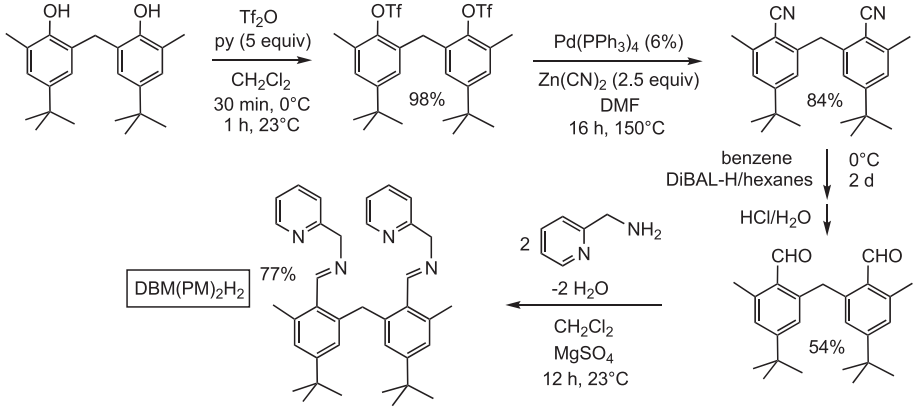

Scheme 3. Synthetic scheme to afford $DBM(PM)_2H_2$, a precursor for reductive coupling.

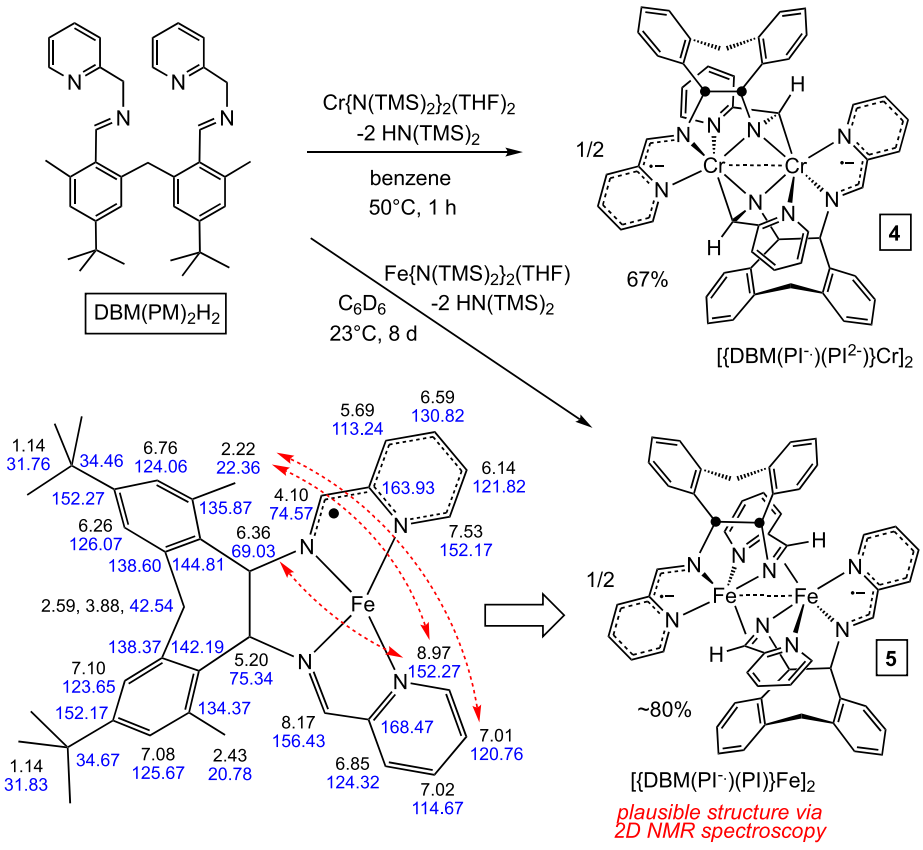

Scheme 4. Syntheses of $[\{DMB(PI)_2\}M]_2$ (M = Cr, **4**; Fe, **5**) based on X-ray crystal structure (**4**) and 2D NMR spectroscopy (**5**). ^1H (black) and ^{13}C (blue) NMR shifts are given, along with correlations based on NOESY measurements. (Color online.)

having upfield shifted resonances. As Scheme 4 illustrates, the basic structure parallels that of the Cr derivative, as it consists of a dimer with no mirror symmetry in the $BDM(PI)_2$ ligand, i.e., $[\{DBM(PI)(PI')Fe\}_2$ (**5**). Crosspeaks from a NOESY spectroscopic experiment show correlations between the methyl and methine protons of the cycloheptane ring to the *ortho* and *meta* protons of the non-reduced pyridine ring, likely only in a dimer similar to **4**. Without metric information, the iron-iron interaction, and the character of the reduced iminopyridine residue cannot be assigned with total confidence. It is likely that some reduction of one PI fragment – drawn as a radical anion in Scheme 4 – and some iron-iron bonding, perhaps augmented by appropriate antiferromagnetic coupling, explains the diamagnetism.

It was hoped that cleaving the dimers in conjunction with oxidants, such as diazo species and azides, would enable the reverse of carbon–carbon bond formation. Storing chemical energy in the form of a bond is an underappreciated and underutilized facet of redox non-innocence [10–19,24–28]. Unfortunately, attempts at cleaving $[\{DBM(PI^{-\cdot})(PI^{2-})\}Cr^{III}]_2$ (**4**) failed or led to degradation, and problems persisted in purifying $[\{DBM(PI)(PI')Fe\}_2$ (**5**), limiting studies of its reactivity.

2.3.3. Structure of $[\{DBM(PI)_2\}Cr]_2$ (**4**)

A molecular view of $[\{DBM(PI)_2\}Cr]_2$ (**4**) is given in Fig. 7, which illustrates the centrosymmetric nature of the dimer, and clearly confirms the *cis*-coupling leading to the dibenzo 7-memebered ring. Each chromium center is coordinated by a pyridine-imine, whose $d(CN_{im})$, $d(CC_{im})$, and $d(CN_{py})$ distances of 1.342(6) Å, 1.398(6) Å, and 1.382(6) Å, respectively, denote the unit as a radical anion [29–32]. The carbon–carbon bond formation (d(C13—C27) = 1.571(6) Å), renders the remaining pyridine-imine as a metalaaziridine, clearly represented by a 1.430(5) Å carbon–nitrogen single bond,[22] and relatively short d(CrC) and d(CrN) of 2.012(3) Å and 2.090(4) Å, respectively. The Cr_2N_2 core is planar, with ∠N2—Cr—N2′ = 87.57(15)° and ∠Cr—N2—Cr′ = 92.43(15)°, and a long dichromium distance of 2.8979(14) Å. The remaining coordination derives from the pyridine (d(Cr—N1 = 2.057(4) Å) attached to the η^2-metalaaziridine. In sum, the metric parameters support a Cr(III) formulation with a weak dichromium interaction, as mentioned above.

3. Conclusions

Chelate ligands featuring azaallyl precursors have provided examples of diimine reductive coupling to form the cyclopropane ring in $Me_2^SPr(cis\text{-}2,3\text{-}NCH_2(2\text{-}py))TiCl_2$ (**1**), and azaallyl coupling to produce the 7-membered rings in $[\{DBM(PI^{-\cdot})(PI^{2-})\}Cr^{III}]_2$ (**4**) and $[\{DBM(PI)(PI')\}Fe]_2$ (**5**). If such ring production can be reversible, the ring-containing chelates can serve in a redox non-innocent capacity. Reversal of the C—C bond formation in **1** would generate a formally Ti(II) center, hence oxidative compensation by a substrate would be likely, but none were observed. Attempts to prepare the free cyclopropanated ligand or its dianionic equivalent were unsuccessful. An interesting byproduct was generated in the magnesium reduction of $Me_2C(CH_2N{=}CH(2\text{-}py))_2$ (dmp(PI)$_2$). Dimeric $[\{Me_2C(CH_2N{=}CH(2\text{-}py))(CH_2(\mu\text{-}N)CH_2(2\text{-}py))\}Mg]_2$ resulted from a monomer that had undergone HAT from an unknown source, possibly THF solvent. It is a rare example of a paramagnetic magnesium complex, whose unpaired spins are localized on separate Mg(iminopyridine) centers and subtly interact. Attempts to reverse

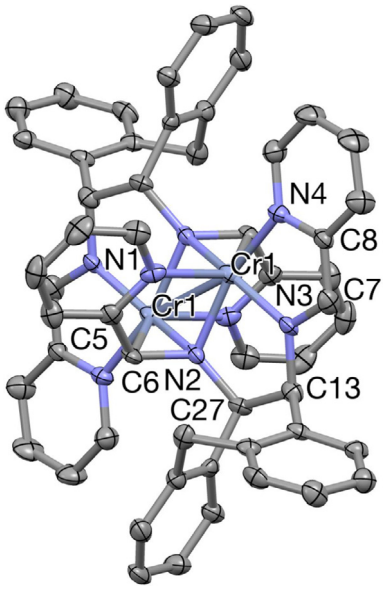

Fig. 7. Molecular view of [{DBM(PI)$_2$}Cr]$_2$ (**4**) with peripheral methyl and ^{t}Bu groups removed. Selected interatomic distances (Å) and angles (°): Cr—Cr, 2.8979 (14); Cr—N1, 2.057(4); Cr—N2, 2.003(4); Cr—N2′, 2.012(3); Cr—N3, 1.929(4); Cr—N4, 2.019(4); Cr—C6, 2.090(4); N2—C6, 1.430(5); N2—C27, 1.513(6); N3—C13, 1.483(6); C5—C6, 1.441(6); C13—C27, 1.571(6); N3—C7, 1.342(6), C7—C8, 1.398(6); N4—C8, 1.382(6); Cr—N2—Cr′, 92.43(15); Cr—N2—C6, 72.9(2); Cr—C6—N2, 66.32(2); N1—Cr—N2, 82.45(15); N1—Cr—N3, 106.96(15); N1—Cr—N4, 97.31(15); N1—Cr—Cr′, 85.98(11); N1—Cr—C6′, 131.63(16); N2—Cr—N2′, 87.57(15); N2—Cr—N3, 82.26(15); N2—Cr—N4, 159.79(16); N2—Cr—C6, 40.82(15), N2—Cr—C6′, 121.32(16); 100.24(16); N2—Cr—Cr′, 43.66(11); N2—Cr′—Cr, 43.91(10); N3—Cr—N4, 78.47(16); N3—Cr′—Cr, 122.93(11); N3—Cr—C6, N4—Cr—Cr′, 156.51(12); N4—Cr—C6, 94.99(16); C6—N2—C27, 126.5(3); N2—C27—C13, 11.8(3); N3—C13—C27, 107.4(4); N3—C7—C8, 114.6(4).

7-membered ring formation in **4** and **5** proved fruitless, as it is likely that interference from concurrent metal–metal bond formation was problematic. Revised ligand systems are currently being explored in order to better exploit reversible ring formation as a redox non-innocent mechanism.

4. Experimental

4.1. General considerations

All manipulations were performed using either glovebox, Schlenk, or high vacuum line techniques, unless stated otherwise. All glassware was oven dried at 180 °C. THF and ether were distilled under nitrogen from purple sodium benzophenone ketyl and vacuum transferred from the same prior to use. Hydrocarbon solvents were treated in the same manner with the addition of 1–2 mL/L tetraglyme. Benzene-d_6 was dried over sodium, vacuum transferred and stored over sodium. THF-d_8 was dried over sodium, and vacuum transferred from sodium benzophenone ketyl prior to use. Acetonitrile-d_3 was dried over refluxing CaH_2, vacuum distilled and stored over CaH_2, and chloroform-d_1 (Cambridge Isotope Laboratories) was used as received. Chelate ligands $Me_2C(CH{=}NCH_2(2\text{-py}))_2$ (dmp(PM)$_2$) and $Me_2C(CH_2N{=}CH(2\text{-py}))_2$ (dmp(PI)$_2$) [1,4,29], (TMEDA)$_2$TiCl$_2$ [20], ^{neo}PeLi [42], Fe(N(TMS)$_2$)$_2$(thf) [41], Cr(N(TMS)$_2$)$_2$(thf)$_2$ [40], and 6,6′-methylenebis (4-(tert-butyl)-2-methylphenol) [39] were prepared according to literature procedures. All other reagents were purchased from various suppliers and used as received.

NMR spectra were obtained using Varian 300 MHz (Mercury), 400 MHz (Inova), 500 MHz (Inova) and 600 MHz (Inova) spectrometers. ^{1}H and ^{13}C NMR shifts are referenced to benzene-d_6 (^{1}H, δ 7.16 ppm; ^{13}C, δ 128.39 ppm), toluene-d_8 (^{1}H, δ 2.09 ppm; ^{13}C, δ 20.40 ppm), acetonitrile-d_3 (^{1}H, δ 1.94 ppm; ^{13}C, δ 118.26 ppm), tetrahydrofuran-d_8 (^{1}H, δ 3.58 ppm; ^{13}C, δ 67.57 ppm), dichloromethane-d_2 (^{1}H, δ 5.32 ppm; ^{13}C, δ 53.84 ppm), deuterium oxide (^{1}H, δ 4.79 ppm; ^{13}C, CH_3CN spike, δ 1.79 ppm). Solution magnetic measurements were conducted via Evans' method [34]. Elemental analyses were performed by Robertson Microlit Laboratories, Madison, New Jersey.

4.2. Procedures

4.2.1. $Me_2^sPr(cis\text{-}2,3\text{-}NCH_2(2\text{-py}))TiCl_2$ (**1**)

A 50 mL round bottom flask was charged with 0.967 g (TMEDA)$_2$TiCl$_2$ (2.75 mmol) and 40 mL C_6H_6. A solution of $Me_2C(ImCH_2Py)_2$ (0.780 g, 2.78 mmol) in C_6H_6 (2 mL) was added dropwise at 23 °C. After stirring for 24 h, about 20 mL of solvent was removed, and the reaction mixture was filtered. The remaining solvent was removed and a light-red solid was dried under vacuum and harvested (1.044 g, 2.38 mmol, 87%). X-ray quality crystals were grown via slow evaporation of a benzene solution. ^{1}H NMR (C_6D_6): δ 1.07 (s, CH_3, 3H), 1.59 (s, CH_3, 3H), 3.13 (s, $^{cPr}CH_2$, 2H), 4.61 (d, J = 21 Hz, CHH, 2H), 4.78 (d, J = 21 Hz, CHH, 2H), 6.51 (d, J = 8 Hz, $^3CH_{py}$, 2H), 6.65 (dd, J = 6, 7 Hz, $^5CH_{py}$, 2H), 6.89 (dd, J = 7, 8 Hz, $^4CH_{py}$, 2H), 8.86 (d, J = 6 Hz, $^6CH_{py}$, 2H). ^{13}C NMR (C_6D_6): δ 13.95 (CH_3), 25.56 (^{cPr}CH), 46.06 ((CH_3)$_2$C), 66.09 (^{cPr}CH), 68.97 (CH_2), 119.97 ($^3C_{py}$), 121.35 ($^5C_{py}$), 136.46 ($^4C_{py}$), 149.18 ($^6C_{py}$), 162.57 (^{im}C).

4.2.2. [{$Me_2C(CH_2N{=}CH(2\text{-py}))(CH_2(\mu\text{-}N)CH_2(2\text{-py}))$}Mg]$_2$ (**3**)

To a 100 mL round bottom flask charged with 2.00 g DMP(PI)$_2$ (7.13 mmol), 387 mg Mg° (~2.25 equiv), and 20.0 mg $HgCl_2$, was vacuum transferred 50 mL THF at −78 °C. The reaction mixture was allowed to warm to 23 °C, and stirred for 48 h. The solution was filtered, the THF removed, and 40 mL pentane was added. The solution was filtered through a medium frit, which was washed with 4 × 5 mL of pentane. Removal of all volatiles afforded 1.150 g (52%; yields varied from 23% to 52%) of red-black **3**. μ_{eff} = 1.8–2.0 μ_B (Evans' Method; C_6D_6, 23 °C, multiple samples). Calc: C, 67.02; H, 6.62; N, 18.39. Found: C, 67.48; H, 6.71; N, 16.79.

4.2.3. Bis(2-triflato-5-(tert-butyl)-3-methylphenyl)methane

To a 100 mL round bottom flask was added 6,6′-methylenebis (4-(tert-butyl)-2-methylphenol) (1.69 g, 5.0 mmol) and pyridine (1.6 mL, 25 mmol, 5 eq.). Upon cooling to 0 °C, a solution of trifluoromethanesulfonic anhydride (2.2 mL, 13.1 mmol, 2.6 eq.) in CH_2Cl_2 (50 mL) was added dropwise over the course of 8 min under an argon atmosphere. The resulting solution was stirred for 30 min, allowed to warm to 23 °C, and stirred for an additional hour. The reaction mixture was quenched with 40 mL of 1.5 M HCl and the layers were separated. The aqueous layer was washed 3x with 30 mL CH_2Cl_2 and the combined organic layers were dried over $MgSO_4$. The solvent was removed in vacuo and pentane (10 mL) was added to the resulting suspension. A white solid was removed via filtration and all volatiles removed in vacuo yielding 2.83 g (4.7 mmol, 94%) of the product as a yellow oil. ^{1}H NMR ($CDCl_3$):δ 1.21 (s, C(CH_3)$_3$, 18H), 2.41 (CH_3), 4.19 (CH_2), 6.88 (s, $^{6\text{-}Ar}CH$, 2H), 7.17 (s, $^{4\text{-}Ar}CH$, 2H). ^{19}F NMR ($CDCl_3$): δ 73.91 (s, CF_3, 6F). ^{13}C NMR ($CDCl_3$):δ 17.69 (CH_3), 31.22 (C(CH_3)$_3$), 31.67 (CH_2), 34.62 (C(CH_3)$_3$), 118.75 (q, J = 320 Hz, CF_3), 126.98 ($^{4\text{-}Ar}CH$), 127.89 ($^{2\text{-}Ar}CH$), 131.13 ($^{3\text{-}Ar}C$), 132.08 ($^{1\text{-}Ar}C$), 144.23 ($^{5\text{-}Ar}C$), 151.32 ($^{2\text{-}Ar}C$).

4.2.4. Bis(2-cyano-5-(tert-butyl)-3-methylphenyl)methane

A 100 mL round bottom flask was charged with bis(2-triflato-5-(tert-butyl)-3-methylphenyl)methane (15.55 g, 25.7 mmol), zinc cyanide (7.20 g, 63.9 mmol, 2.5 eq), and Pd(PPh$_3$)$_4$ (1.7 g, 1.5 mmol, 6 mol %). DMF (15 mL) was added under argon purge and the system was set to reflux for 16 h. Upon cooling the solid residue was

crushed and suspended in 200 mL H_2O. This suspension was extracted 3× with 100 mL $CHCl_3$ and the combined organic layers were stripped of volatiles *in vacuo*. The solid was dissolved in CH_2Cl_2 and filtered through a pad of Celite. The solvent was removed *in vacuo* to yield an off-white solid which was washed with 50 mL cold (−78 °C) pentane. Drying the resulting white powder yielded 7.72 g (21.5 mmol, 84%) of the bis(nitrile). ^{1}H NMR ($CDCl_3$): δ 1.27 (s, $C(CH_3)_3$, 18H), 2.54 (s, CH_3, 6H), 4.37 (s, CH_2, 2H), 7.34 (s, $^{6\text{-Ar}}$CH, 2H), 7.36 (s, $^{4\text{-Ar}}$CH, 2H).

4.2.5. 6,6′-Methylenebis(4-(tert-butyl)-2-methylbenzaldehyde)

To a 50 mL round bottom flask charged with bis(2-cyano-5-(tert-butyl)-3-methylphenyl)-methane (1.20 g, 3.3 mmol) was added 25 mL benzene via vacuum-transfer. A solution of DIBAL-H in hexanes (10 mL, 10 mmol, 3 eq) was added dropwise at 0 °C and the solution was stirred for 2 d. Aqueous HCl (10 mL, 1 M) was added dropwise, and gas evolution, and a color change from yellow to pink and then back to yellow was noted. The organic layer was concentrated by half and 4 mL concentrated HCl was added. The mixture was stirred rapidly and refluxed for 2 h. Upon cooling the organic layer was separated, dried over Na_2SO_4, and the solvent removed in vacuo yielding 0.643 g of dialdehyde (1.6 mmol, 54%). ^{1}H NMR (C_6D_6): δ 1.09 (s, $C(CH_3)_3$, 18H), 2.40 (s, CH_3, 6H), 4.79 (s, Ar_2CH_2, 2H), 6.94 (s, $^{6\text{-Ar}}$CH, 2H), 6.95 (s, $^{4\text{-Ar}}$CH, 2H), 10.47 (s, ArCHO, 2H). ^{13}C NMR (C_6D_6): δ 21.20 (CH_3), 31.22 ($C(CH_3)_3$), 35.19 ($C(CH_3)_3$), 37.37 (CH_2), 127.12 ($^{5\text{-Ar}}$CH), 127.65 ($^{3\text{-Ar}}$CH), 130.97 ($^{1\text{-Ar}}$C), 141.87 ($^{6\text{-Ar}}$C), 143.79 ($^{2\text{-Ar}}$C), 156.47 ($^{4\text{-Ar}}$C), 192.56 (CHO).

4.2.6. ((Methylenebis(4-(tert-butyl)-2-methyl-6,1-phenylene))bis(methanyl-ylidene))bis(1-(pyridin-2-yl)methanamine) (DBM(PM)$_2$H$_2$)

Bis(2-carboxaldehyde-5-(tert-butyl)-3-methylphenyl)methane (0.600 g, 1.6 mmol) was added to a 20 mL scintillation vial with 2 mL CH_2Cl_2 and a solution of aminomethylpyridine (0.540 g, 5 mmol, 3 eq.) was added dropwise. Solid $MgSO_4$ (0.300 g, 2.5 mmol) was added in one portion and the suspension was stirred for 12 h. The suspension was filtered and the filter cake was washed with CH_2Cl_2. The solvent was removed in vacuo and the solid was crushed and suspended in cold (−40 °C) pentane. The supernatant was decanted and the residue dried to yield 0.740 g (1.4 mmol, 77%) as a white solid. ^{1}H NMR (C_6D_6): δ 1.19 (s, $C(CH_3)_3$, 18H), 2.48 (s, CH_3, 6H), 4.73 (s, Ar_2CH_2, 2H), 4.94 (s, CH_2, 4H), 6.62 (dd, J = 4.7, 7.5 Hz, $^{5\text{-py}}$CH, 2H), 7.10 (s, $^{6\text{-Ar}}$CH, 2H), 7.10 (t, J = 7.5 Hz, $^{4\text{-py}}$CH, 2H), 7.12 (s, $^{4\text{-Ar}}$CH, 2H), 7.20 (d, J = 7.5 Hz, $^{3\text{-py}}$CH, 2H), 8.48 (d, J = 4.7 Hz, $^{6\text{-py}}$CH, 2H), 8.71 (s, $^{\text{im}}$CH, 2H).

4.2.7. Bis[3,7-di-tert-butyl-1,9-dimethyl-N10,N11-bis(pyridin-2-ylmethylene)-10,11-dihydro-5H-dibenzo[a,d][7]annulene-10,11-diamine]dichromium, [{DBM(PI$^{\bullet-}$)(PI^{2-})}Cr^{III}]$_2$ (**4**)

A small bomb reactor was charged with a solution of DBM(PM)$_2$H$_2$ (0.245 g, 0.45 mmol) in 5 mL C_6H_6 and a solution of Cr(N(TMS)$_2$)$_2$(THF)$_2$ (0.233 g, 0.45 mmol) in 5 mL C_6H_6 was added dropwise. The color changed from light lavender to purple, then brown/green, and finally red over the course of a few minutes. The bomb was sealed and stirred in a 50 °C oil bath for 1 h. The solvent was removed *in vacuo* and the residue was triturated with pentane to yield a red-brown powder (178 mg, 0.30 mmol, 67%); red-black crystals were obtained from THF. μ_{eff} = 3.8 μ_B (Evans' method, C_6D_6, 23 °C).

4.3. NMR tube scale reactions

4.3.1. Me$^{\varsigma}$Pr(cis-2,3-NCH$_2$(2-py))Ti(^{neo}Pe)$_2$ (**2**)

An NMR tube was charged with **1** (30 mg, 0.068 mmol), NpLi (11 mg, 0.14 mmol, 2.1 eq.) and C_6D_6 (0.5 mL). After 2 d at 23 °C, near quantitative formation of **2** was observed according to ^{1}H NMR spectral analysis. ^{1}H (C_6D_6): δ 0.69 (s, CH_3, 9H), 0.74 (s, CH_2, 2H), 0.78 (s, CH_2, 2H), 0.86 (s, CH_3, 9H), 1.27 (s, CH_3, 3H), 1.57 (s, CH_3, 3H), 3.00 (s, $^{\text{cPr}}$CH, 2H), 4.76 (d, J = 21 Hz, CHH, 2H), 5.12 (d, J = 21 Hz, CHH, 2H), 6.75 (dd, J = 5.5, 7.5 Hz, ^{5}CH$_{py}$, 2H), 6.77 (d, J = 7.5 Hz, ^{3}CH$_{py}$, 2H), 7.00 (t, J = 7.5 Hz, ^{4}CH$_{py}$, 2H), 8.63 (d, J = 5.5 Hz, ^{6}CH$_{py}$, 2H).

4.3.2. Bis[3,7-di-tert-butyl-1,9-dimethyl-N10,N11-bis(pyridin-2-ylmethylene)-10,11-dihydro-5H-dibenzo[a,d][7]annulene-10,11-diamine]diiron, [{DBM(PI)(PI$^{\prime}$)}Fe]$_2$ (**5**)

DBM(PM)$_2$H$_2$ (10 mg, 0.02 mmol) in C_6D_6 (0.3 mL) was added to a solution of Fe(N(TMS)$_2$)$_2$(THF) (8 mg, 0.02 mmol) in C_6D_6 (0.3 mL) in an NMR tube and sealed. The solution turned green upon thawing and turned red within five minutes, at which time HMDS and THF were visible in the ^{1}H NMR spectrum (~1:1 ratio, respectively), amongst several paramagnetic resonances. After 8 d at 23 °C, there was nearly complete (>80%) conversion to a new diamagnetic product (all peaks have $\nu_{1/2} \geq$10 Hz). Spectral characteristics were determined by gCOSY, ^{13}C NMR, ROESY, and HSQCAD spectroscopies. ^{1}H (C_6D_6): δ 1.14 (s, ^{30}CH$_3$ and ^{32}CH$_3$, 18H), 2.22, (s, ^{33}CH$_3$, 3H), 2.43 (s, ^{28}CH$_3$, 3H), 2.59 (d, J = 12 Hz, ^{14}CHH, 1H), 3.88 (d, J = 12 Hz, ^{14}CHH, 1H), 4.10 (s, ^{22}CH, 1H), 5.20 (s, ^{7}CH, 1H), 5.69 (s, ^{24}CH, 1H), 6.14 (s, ^{26}CH, 1H), 6.26 (s, ^{16}CH, 1H), 6.36 (s, ^{21}CH, 1H), 6.59 (s, ^{25}CH, 1H), 6.76 (s, ^{18}CH, 1H), 7.53 (s, ^{27}CH, 1H), 8.17 (s, ^{6}CH, 1H), 8.97 (s, ^{1}CH, 1H). ^{13}C (C_6D_6): δ 20.78 (^{28}CH$_3$), 22.36 (^{33}CH$_3$), 31.76 (^{32}CH$_3$), 31.83 (^{30}CH$_3$), 34.46 (^{31}C(CH$_3$)$_3$), 34.67 (^{29}C(CH$_3$)$_3$), 42.54 (^{14}CH$_2$), 69.03 (^{21}CH), 74.57 (^{22}CH), 75.34 (^{7}CH), 113.24 (^{24}CH), 114.67 (^{3}CH), 120.76 (^{2}CH), 121.82 (^{27}CH), 123.65 (^{12}CH), 124.06 (^{18}CH), 124.32 (^{4}CH), 125.67 (^{10}CH), 130.82 (^{25}CH), 134.37 (^{9}C), 135.87 (^{19}C), 138.37 (^{13}C), 138.60 (^{15}C), 142.19 (^{8}C), 144.81 (^{20}C), 149.25 (^{11}C), 150.31 (^{17}C), 152.17 (^{27}CH), 152.27 (^{1}CH), 156.43 (^{6}CH). See below for the numbering scheme.

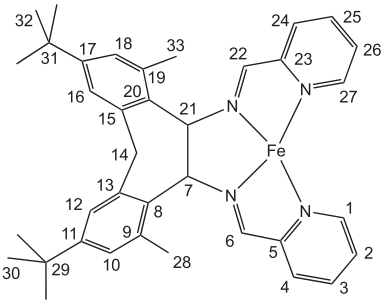

4.4. X-ray crystal structure determinations

4.4.1. Me$^{\varsigma}$Pr(cis-2,3-NCH$_2$(2-py))TiCl$_2$ (**1**)

A red plate measuring 0.35 × 0.15 × 0.05 mm^3 was obtained from benzene. Crystal data for $C_{20}H_{23}N_4Cl_2Ti$, M = 438.22, monoclinic, $P2_1/n$, a = 10.0514(4), b = 15.4640(6), c = 13.5561(4) Å, β = 94.3730(10)°, V = 2100.96(13) Å^3, T = 173(2) K, λ = 0.71073 Å, Z = 4, ρ_{calc} = 1.385 Mg/m^3, μ = 0.674 mm^{-1}, 24 059 reflections, 6409 independent (R_{int} = 0.0294), R_1 (all data) = 0.0483, wR_2 = 0.0810, R_1 ($I > 2\sigma I$)) = 0.0318, wR_2 = 0.0732, *GOF* = 1.010.

4.4.2. [{Me$_2$C(CH$_2$N=CH(2-py))(CH$_2$(μ-N)CH$_2$(2-py))}Mg]$_2$ (**3**)

A red-black plate measuring 0.50 × 0.20 × 0.05 mm^3 was obtained from pentane. Crystal data for $C_{34}H_{42}N_8Mg_2$, M = 611.38, monoclinic, $P2_1/c$, a = 10.5580(4), b = 13.7124(7), c = 11.8057(4) Å, β = 94.564(3)°, V = 1694.30(14) Å^3, T = 203(2) K, λ = 0.71073 Å,

$Z = 2$, $\rho_{calc} = 1.198$ Mg/m^3, $\mu = 0.107$ mm^{-1}, 15 019 reflections, 4362 independent ($R_{int} = 0.0262$), R_1 (all data) = 0.0598, $wR_2 = 0.1145$, R_1 ($I > 2\sigma I$)) = 0.0394, $wR_2 = 0.0996$, $GOF = 1.028$.

4.4.3. [{DBM(PI$^{-\cdot}$)(PI^{2-})}Cr^{III}]$_2$ (**4**)·THF$_2$

A black block measuring 0.25 × 0.20 × 0.15 mm^3 was obtained from THF. Crystal data for $C_{90}H_{116}N_8O_4Cr_2$, $M = 1477.90$, triclinic, $P\bar{1}$, $a = 9.9818(8)$, $b = 13.6414(11)$, $c = 15.5199(4)$ Å, $\beta = 78.482(3)^\circ$, $V = 2017.5(3)$ Å^3, $T = 173(2)$K, $\lambda = 0.71073$ Å, $Z = 1$, $\rho_{calc} = 1.216$ Mg/m^3, $\mu = 0.325$ mm^{-1}, 19 149 reflections, 4899 independent ($R_{int} = 0.0922$), R_1 (all data) = 0.1068, $wR_2 = 0.1531$, R_1 ($I > 2\sigma I$)) = 0.0590, $wR_2 = 0.1299$, $GOF = 1.047$.

4.5. Computational methods

Density Functional Theory (DFT) calculations were performed with version 4.002 of the ORCA software package [1]. Calculations of Me_2^SPr(*cis*-2,3-NCH$_2$(2-py))TiCl$_2$ (**1**) and its ring-opened isomer **1′** employed coordinates optimized using the BP86 functional [2,3], the scalar-relativistically recontracted ZORA-def2-TZVP(-f) [4] basis set on all atoms, and solvation was modeled using the conductor-like polarizable continuum model (CPCM) [5] with a dielectric of 9.08 (CH_2Cl_2). Optimizations were carried out along a continuum of C7–C8 distances from 1.35 to 2.65 Å using three limiting formalisms: spin-restricted (singlet), spin-unrestricted (triplet), and broken symmetry (BS 1,1) [6]. Structures obtained at the singlet minimum (1.45 Å) and triplet minimum (2.45 Å) were used for subsequent single point calculations. Calculations of [{Me$_2$C(CH$_2$N=CH(2-py))(CH$_2$(μ-N)CH$_2$(2-py))}Mg]$_2$ (**3**) employed crystallographic coordinates. Single-point energies were calculated by using the B3LYP [7] functional and the RIJCOSX algorithm to speed the calculation of Hartree–Fock exchange [8]. The scalar relativistically recontracted Ahlrich's ZORA-def2-TZVP(−f) basis set [4] with ORCA Grid4 was used for all atoms. Calculations included the zeroth-order regular approximation (ZORA) [9] for relativistic effects as implemented by van Wüllen [10]. Solvation was modeled with CPCM in a dielectric of 9.08 (CH_2Cl_2) [5].

Acknowledgements

Support from the National Science Foundation (CHE-1402149, CHE-1664580 (PTW), CHE-1454455 (KML)) and Cornell University is gratefully acknowledged. NSF support for the CCB NMR facility (NSF-MRI CHE-1531632) is appreciated, as is technical aid from Ivan Keresztes. We also acknowledge Samantha N. MacMillan for aid in X-ray crystallographic studies.

Appendix A. Supplementary data

CCDC 1861255, 1861257, and 1861256 contains the supplementary crystallographic data for Me$_2$Pr(*cis*-2,3-NCH$_2$(2-py))TiCl$_2$ (**1**), [{Me$_2$C(CH$_2$N=CH(2-py))(CH$_2$(μ-N)CH$_2$(2-py))}Mg]$_2$, and [{DBM(PI$^{-\cdot}$)(PI^{2-})}Cr^{III}]$_2$ (**4**)·THF$_2$, respectively. These data can be obtained free of charge via http://www.ccdc.cam.ac.uk/conts/retrieving.html, or from the Cambridge Crystallographic Data Centre, 12 Union Road, Cambridge CB2 1EZ, UK; fax: (+44) 1223-336-033; or e-mail: deposit@ccdc.cam.ac.uk.

References

[1] E.B. Hulley, P.T. Wolczanski, E.B. Lobkovsky, J. Am. Chem. Soc. 133 (2011) 18058.
[2] B.A. Frazier, V.A. Williams, P.T. Wolczanski, S. Bart, K. Meyer, T.R. Cundari, E.B. Lobkovsky, Inorg. Chem. 52 (2013) 3295.
[3] W.D. Morris, P.T. Wolczanski, J. Sutter, K. Meyer, T.R. Cundari, E.B. Lobkovsky, Inorg. Chem. 53 (2014) 7467.
[4] E.B. Hulley, E.B.V.A. Williams, W.D. Morris, P.T. Wolczanski, K. Hernández-Burgos, E.B. Lobkovsky, T.R. Cundari, Polyhedron 84 (2014) 182.
[5] B.A. Frazier, P.T. Wolczanski, I. Keresztes, S. DeBeer, E.B. Lobkovsky, A.W. Pierpont, T.R. Cundari, Inorg. Chem. 51 (2012) 8177.
[6] E.C. Volpe, P.T. Wolczanski, J.M. Darmon, E.B. Lobkovsky, Polyhedron 52 (2013) 406.
[7] B.L. Lindley, P.T. Wolczanski, T.R. Cundari, E.B. Lobkovsky, Organometallics 34 (2015) 4656.
[8] B.P. Jacobs, P.T. Wolczanski, E.B. Lobkovsky, Inorg. Chem. 55 (2016) 4223.
[9] S.P. Heins, W.D. Morris, T.R. Cundari, S.N. MacMillan, E.B. Lobkovsky, N. Livezey, P.T. Wolczanski, Organometallics 37 (2018), https://doi.org/10.1021/acs.organomet.8b00188.
[10] F. Fransceschi, E. Solari, R. Scopelliti, C. Floriani, Angew. Chem. Int. Ed. 45 (2000) 1685.
[11] E. Gallo, E. Solari, N. Re, C. Floriani, A. Chiesi-Villa, C. Rizzoli, J. Am. Chem. Soc. 119 (1997) 5144.
[12] S. Gambarotta, C. Floriani, A. Chiesi-Villa, C. Guastini, J. Chem. Soc., Chem. Commun. (1982) 756.
[13] S. Gambarotta, M. Mazzanti, C. Floriani, M.A. Zehnder, J. Chem. Soc., Chem. Commun. (1984) 1116.
[14] S. Gambarotta, F. Urso, C. Floriani, A. Chiesi-Villa, C. Guastini, Inorg. Chem. 22 (1983) 3966.
[15] R. Crescenzi, E. Solari, C. Floriani, A. Chiesi-Villa, C. Rizzoli, J. Am. Chem. Soc. 121 (1999) 1695.
[16] J. Jubb, C. Floriani, A. Chiesi-Villa, C. Rizzoli, J. Am. Chem. Soc. 114 (1992) 6571.
[17] S. De Angelis, E. Solari, C. Floriani, A. Chiesi-Villa, C. Rizzoli, J. Am. Chem. Soc. 116 (1994) 5702.
[18] U. Piarulli, E. Solari, C. Floriani, A. Chiesi-Villa, C. Rizzoli, J. Am. Chem. Soc. 118 (1996) 3634.
[19] R. Crescenzi, E. Solari, C. Floriani, A. Chiesi-Villa, C. Rizzoli, Inorg. Chem. 37 (1998) 6044.
[20] J.J.H. Edema, R. Duchateau, S. Gambarotta, R. Hynes, E. Gabe, Inorg. Chem. 30 (1991) 154.
[21] J.J.H. Edema, W. Stauthamer, F. Van Bolhuis, S. Gambarotta, W.J.J. Smeets, A.L. Spek, Inorg. Chem. 29 (1990) 1302.
[22] F.H. Allen, O. Kennard, D.G. Watson, L. Brammer, A.G. Orpen, R. Taylor, J. Chem. Soc. Perkin Trans. I I (1987) S1.
[23] A.A. Zavitsas, J. Phys. Chem. A. 107 (2003) 897.
[24] J. Bachmann, D.G. Nocera, J. Am. Chem. Soc. 126 (2004) 2829.
[25] J. Bachmann, D.G. Nocera, J. Am. Chem. Soc. 127 (2005) 4730.
[26] J. Bachmann, J.M. Hodgkiss, E.R. Young, D.G. Nocera, Inorg. Chem. 46 (2007) 607.
[27] J. Bachmann, T.S. Teets, D.G. Nocera, Dalton Trans. 34 (2008) 4549.
[28] D. Bhattacharya, S. Maji, K. Pal, S. Sarkar, Inorg. Chem. 48 (2009) 6362.
[29] V.A. Williams, E.B. Hulley, P.T. Wolczanski, K.M. Lancaster, E.B. Lobkovsky, Chem. Sci. 4 (2013) 3636.
[30] C.C. Lu, E. Bill, T. Weyhermüller, E. Bothe, K. Wieghardt, J. Am. Chem. Soc. 130 (2008) 3181.
[31] A.A. Trifonov, E.A. Fedorova, I.A. Borovkov, G.K. Fukin, E.V. Baranov, J. Larionova, N.O. Druzhkov, Organometallics 26 (2007) 2488.
[32] A. Mondal, T. Weyhermüller, K. Wieghardt, Chem. Commun. (2009) 6098.
[33] T.W. Myers, T.J. Sherbow, J.C. Fettinger, L.A. Berben, Dalton Trans. 45 (2016) 5989.
[34] (a) D.F. Evans, J. Chem. Soc. (1959) 2003;
(b) E.M. Schubert, J. Chem. Educ. 69 (1992) 62.
[35] B.N. Figgis, M.A. Hitchman, Ligand Field Theory and Its Applications, Wiley-VCH, New York, 2000.
[36] A.W. Addison, T. Nageswara Rao, J. van Rijn, G.C. Verschoor, Dalton Trans. (1984) 1349.
[37] (a) B.A. Frazier, E.R. Bartholomew, P.T. Wolczanski, S. DeBeer, M. Santiago-Berrios, H.D. Abruña, E.B. Lobkovsky, S.C. Bart, S. Mossin, K. Meyer, T.R. Cundari, Inorg. Chem. 50 (2011) 12414;
(b) B.A. Frazier, P.T. Wolczanski, E.B. Lobkovsky, T.R. Cundari, J. Am. Chem. Soc. 131 (2009) 3428.
[38] B.A. Frazier, P.T. Wolczanski, E.B. Lobkovsky, Inorg. Chem. 48 (2009) 11576.
[39] M. Aoki, K. Nakashima, H. Kawabata, S. Tsutui, S. Shinkai, J. Chem. Soc., Perkin Trans. 2 (3) (1999) 347.
[40] (a) D.C. Bradley, M.B. Hursthouse, C.W. Newing, A.J. Welch, J. Chem. Soc., Chem. Commun. (1972) 567;
(b) B. Horvath, J. Strutz, E.G. Horvath, Für Anorg. Allg. Chem. 457 (1979) 38.
[41] (a) M.M. Olmstead, P.P. Power, S.C. Shoner, Inorg. Chem. 30 (1991) 2547;
(b) R.A. Andersen, K. Faegri, J.C. Green, A. Haaland, M.F. Lappert, W.P. Leung, K. Rypdal, Inorg. Chem. 27 (1988) 1782;
(c) H. Bürger, U. Wannagat, Monatsh. Chem. 94 (1963) 1007.
[42] S. Kyushin, M. Ikarugi, K. Takatsuna, M. Goto, H. Matsumoto, J. Organomet. Chem. 510 (1996) 121.